

FABRICATION OF BIOCOMPATIBLE NANO-CARBONATED HYDROXYAPATITE/POLYMER SPONGY SCAFFOLDS

S. A. SIDDIQI^{a*}, U. AZHAR^a, F. MANZOOR^a, A. JAMAL^a, M. TARIQ^b,
M. SALEEM^c, A. A. CHAUDHRY^a, I. U. REHMAN^{a, d}

^a*Interdisciplinary Research Centre in Biomedical Materials (IRCBM), COMSATS Institute of Information Technology, Defence Road, Off Raiwind Road, Lahore-54600, Pakistan.*

^b*Department of Biology, Syed Babar Ali School of Science and Engineering, LUMS, DHA, Lahore 54792, Pakistan*

^c*Department of Physics, Syed Babar Ali School of Science and Engineering, LUMS, DHA, Lahore 54792, Pakistan*

^d*Department of Material Science and Engineering, The Kroto Research Institute, University of Sheffield, Broad Lane, S3 7HQ, Sheffield, UK*

Spongy scaffolds containing nano-carbonated hydroxyapatite (nCHA), with compositions $\text{Ca}_{10}(\text{PO}_4)_{6-y}(\text{CO}_3)_y(\text{OH})_2$, with $y=0,2,4$, were prepared by the lyophilization method using different polymers such as natural gelatin (GE), chitosan (CS) and polyvinyl alcohol (PVA), alone or in their combinations. The samples were characterized by using XRD, SEM, and FTIR techniques. All the scaffolds were found to have porosities above 70% and their morphology changed significantly for one nCHA/polymer combination to the other. The nCHA containing scaffolds mediated cytotoxicity (MTT assay) and cell attachment studies were carried out on rat bone marrow derived mesenchymal stem cells (rMSC). Evident cell attachment and no significant cytotoxicity was observed. The preparation of spongy scaffolds and their biocompatibility augment their potential use in tissue engineering and biomedical applications.

(Received February 8, 2018; Accepted April 25, 2018)

Keywords: Nano-carbonated hydroxyapatite, Spongy scaffolds, Mesenchymal stem cells, Hydroxyapatite/polymer scaffolds, MTT Assay, Biocompatibility

1. Introduction

One of the key challenges in producing synthetic bone substitutes is to mimic the chemical composition and microstructure of natural bone material. The human bone is a composite of inorganic and organic components. The inorganic component of human bone is chemically similar to synthetic hydroxyapatite (HA), $\text{Ca}_{10}(\text{PO}_4)_6(\text{OH})_2$ with Ca/P ratio of 1.67. This is also known as biological apatite and contains up to 4-8% carbonate and additionally many other ionic components such as Si, Mg, K, Sr, Zn etc, whose maximum weight composition is up to 4% [1, 2]. It is now well established that the carbonate substituted hydroxyapatite (CHA) is osteophilic as compared to carbonate free HA. The traditional methods for the synthesis of highly porous structures, or scaffolds, involve sintering at temperatures above 1200°C but this causes the loss of carbonate content which in itself is a much-desired component of the bone composition. Therefore, some new methods of scaffolds synthesis are being devised that ensure the stability of carbonate in HA after processing.

Human bones deteriorate by osteoporosis due to aging and menopause. Additionally, accident, trauma, infection, and tumor resection also induce bone defects, which require repair in large quantities all over the world. For example, about 4.5 million to 6.3 million receive orthopedic medical attention each year in the United States alone [3]. The average citizen in a developed country can expect to sustain two fractures over the course of their lifetime. Therefore, to repair

the damaged bone, artificial bone-graft substitutes and porous scaffolds identical to natural bone in porosity, density, and biomechanical properties are required and this area has been the subject of intense global research in recent years.

A basic requirement for the synthesized scaffolds is that they should have the right sized interconnected pores so that re-sorbable bone growth and replacement may take place mimicking natural growth processes. Hutmacher and his co-workers have contributed significant literature on the structural design of scaffolds, pore sizes and interconnectivity, matrix material and their mechanical properties from the point of view of their tissue engineering applications in bone regeneration[4, 5]. Biological apatite may contain up to 8wt% carbonate ions that occupy phosphate and hydroxide positions in the lattice[2]. The presence of these ions produces structural disorder which helps in improving HA bonding to surrounding tissue as a result of higher solubility. HA is used as a bone graft substitute, reinforcement in composites, porous scaffold and bioactive coatings etc [6, 7] whereas carbonate-hydroxyapatite (CHA) is a main hard tissue component, as present in dental enamel[8] as well.

HA has excellent biocompatibility with synthetic and natural polymers[9, 10]. The HA-polymer composite is a simple physical mixture. It is used to enhance the mechanical properties and bioactivity of bio ceramics and polymeric composites with applications in bone tissue engineering [10-13]. It is also reported that addition of polymer in HA could improve the activity, viability of cell culture and improve the cell attachment properties of the alginate scaffolds[14].

The various kinds of ceramic/polymer composite such as HA/collagen [15, 16], HA/gelatin(GE)[1, 10], HA/chitosan (CS)[11, 17], HA/collagen/Poly-lactic acid[18], have already been employed for preparing scaffolds for tissue engineering. GE as a binding agent seems to be quite attractive because it is derived from collagen and contains useful biological functional groups, such as amino acids which can enhance cell growth. CS is biocompatible, biodegradable and its degradation is nontoxic; hence it can be obtained by partially deacetylation of chitin which can be extracted from crustacean [19]. Polyvinyl alcohol (PVA) is the most commonly used polymer for biomedical applications and possesses a hydroxyl group on every second carbon atom. The high concentration of hydroxyl groups makes PVA physically crosslink without the incorporation of any chemical additive[20].

The use of nano-HA instead of micro-sized HA in improving the bioactivity in bone tissue engineering has been the subject of several recent studies[21]. Freeze drying is a simple technique that can produce even complex-shaped and highly porous ceramic or polymeric scaffolds. The requirements for an ideal scaffold include non-toxicity, biocompatibility, suitable mechanical strength, biodegradability with appropriate rate, and should not have any adverse effects on the surrounding tissues and organs. Furthermore, it should have high porosity and interconnected pores to provide sufficient space for the cells, their seeding, growth and proliferation. With these requirements in mind, we report the synthesis of porous scaffolds of nCHA with different biologically acceptable polymers (GE, PVA, and CS) and explore their viability for biomedical applications.

2. Materials and methods

Calcium nitrate tetrahydrate $\text{Ca}(\text{NO}_3)_2 \cdot 4\text{H}_2\text{O}$, 99%, Urea $(\text{NH}_2)_2\text{CO}$, 99.5% were supplied by Riedel-deHaen, Di-ammonium hydrogen phosphate, $(\text{NH}_4)_2\text{HPO}_4$, 96% was supplied by Applichem. Ammonium hydroxide solution (NH_4OH , $\geq 30\%$ w/w) was used to adjust pH of the solution. Analytical grade Gelatin (GE) powder was supplied from Fluka, Germany. PVA ($M_w=72,000$) was supplied by Merck and chitosan (CS) powder with 81% degree of deacetylation (DD), ($M_w=88\text{kDa}$) was extracted from shrimp shells.

Synthesis of nano-Carbonate Substituted Hydroxyapatite (nCHA)

Calcium nitrate tetra-hydrate solution and di-ammonium hydrogen phosphate (DAHP)/urea solutions were prepared in distilled water separately. The pH of both solutions was brought to about 11 by the addition of ammonium hydroxide solution. Then urea-DAHP solution was added drop wise into calcium nitrate solution while the pH was maintained above 11. The reaction

mixture was allowed to stir for 30 minutes and then the solution was transferred to PTFE autoclave with a stainless steel outside container. The autoclave was put into the drying oven at 100°C for 4 h for hydrothermal treatment. The resulting mixture was filtered and washed until the pH of the solution became 7. The sample was dried in a drying oven at 80°C for 24-hours and the precipitates were ground in a pestle-mortar. Subsequently CHA powders were prepared in two compositions of carbonate with Y=0, 2, 4 in $\text{Ca}_{10}(\text{PO}_4)_{6-y}(\text{CO}_3)_y(\text{OH})_2$ for the preparation of scaffolds.

Preparation of Gelatin/ Carbonated-HA scaffolds

GE powder was poured into 40 ml distilled water at 40°C with constant stirring for 6h. Pre-prepared nCHA, $\text{Ca}_{10}(\text{PO}_4)_{6-y}(\text{CO}_3)_y(\text{OH})_2$ with y=0,2,4, were separately added into the GE solution using the weight ratio of GE/nCHA as 1/1 and milky slurries of nCHA and GE were obtained by constant stirring. The slurries were poured into 24-well plate templates and frozen at -40°C for 2 h. Furthermore, the samples were transferred into freeze-drier for lyophilization for 24 h.

Preparation of PVA/ Carbonated-HA scaffolds

Similarly PVA (Merck $M_w=72,000$) was dissolved in 40ml distilled water at 90°C with constant stirring for 6h. Pre-prepared nCHA, $\text{Ca}_{10}(\text{PO}_4)_{6-y}(\text{CO}_3)_y(\text{OH})_2$ with y=0,2,4 were added, one by one, into PVA transparent solution using the weight ratio of PVA/nCHA as 1/1 with constant stirring to obtain a milky slurry of nCHA and PVA. The slurries were poured into 24-well plate templates and kept at -40°C for 2h in a freezer. Subsequently, the samples were placed in a freeze-drier for lyophilization for 24 h.

Preparation of Chitosan/ Carbonated-HA scaffolds

Similarly, CS powder was dissolved in distilled water at 50°C with constant stirring for 6h. 1% acetic acid was added to enhance CS dissolution. Similarly, pre-prepared nCHA, with y=0,2,4, were added to CS solutions, separately prepared, using the weight ratio of CS/nCHA as 1/1 with constant stirring to obtain milky slurries of nCHA and CS. The slurries were poured into 24-well plate templates and frozen at -40°C for 2h in a freezer. Subsequently the samples were freeze-dried for lyophilization for 24 h.

Preparation of PVA/Chitosan/ Carbonated-HA scaffolds

Pre-prepared PVA and CS solutions were mixed together at room temperature using the weight ratio of (PVA/CS/nCHA) as 1/1/2 for 6h. Pre-prepared nCHA, powders, with y=0,2,4, were added to PVA and CS solutions using the similar (polymer/nCHA) weight ratio with constant stirring to obtain a milky slurry of nCHA, PVA and CS. The slurries were poured into 24-well plate template and frozen at -40°C for 2h. Subsequently, the samples were lyophilized for 24 h.

In vitro culture of rat mesenchymal stem cells (MSC)

Rat mesenchymal stem cells (rMSC) were isolated from the femur of 4-5 weeks' rats using the direct adherence method [22, 23]. The femur was isolated under sterile conditions. A disposable aseptic syringe was used to draw antibiotic supplemented L-DMEM (Gibco) medium and to repeatedly fill bone marrow cavity to collect cells in a sterile petri dish. The obtained cell suspension was centrifuged at 250xg for 5 minutes. The cell pellet was re-suspended in DMEM containing 10% FBS (Gibco) and 0.1% penicillin and streptomycin (Gibco) and transferred to T25 tissue culture flask. The flasks were incubated at 37 deg. C in a 5 % CO₂ incubator. Cells isolated from one rat were cultured in one flask. The first medium was changed after 4 days. Later, the medium was changed on alternative days until the cells become 70–80 % confluent. MSC were sub-cultured at 70–80 % confluence. The cells were trypsinized, counted (dead cells excluded by trypan blue assay) and passaged in T-75 flasks. Second- or third-passage MSC were used for cytotoxicity and SEM analysis. In the present study, all cell culture experiments were performed in compliance with the Biosafety, Ethical Rules and Regulations administered by the Ethical Committee of Animal Handling for Experimentation, University of Veterinary and Animal Sciences, Lahore. All the experiments were approved by the Ethical Review Committee for the

Use of Laboratory Animals (ERCULA), University of Veterinary and Animal Sciences (UVAS), Pakistan. The reported study was restricted to rats and no human trials or experiments were performed.

MTT Assay

Cellular toxicity was determined by 3-(4,5-Dimethylthiazol-2-yl)-2,5-diphenyltetrasodium bromide (MTT) assay. Prior to cell culture, all the scaffolds were sterilized with ethanol. Immediately before cell seeding, the scaffolds were washed 2-3 times with PBS and pre-conditioned in DMEM medium for an hour. MSC were seeded in 24-well cell culture plate with 5×10^4 cells per well with or without scaffolds. Cells seeded in 24-plate wells without scaffold were used as positive control. Post day 7 the medium was discarded and cells/scaffolds were washed with 1 ml PBS. 1 ml (0.5 mg/ml) MTT solution was added to each well and the plate was incubated at 37°C for 3 hrs. The MTT solution was discarded and the cells/scaffolds were washed once with 1 ml PBS. To solubilize the formazan crystals 0.5 ml dimethyl sulfoxide (DMSO) was added to each well and the plate was kept under shaking for 15-20 minutes. The optical density (OD) of the dissolved crystals was measured by using micro plate reader at 590 nm. The assay was set up in triplicate with MSC derived from 3 different rats for each sample. The percentage viability is represented as mean \pm SD of 3 independent experiments.

Cell Attachment

To examine the cell attachment capacity on to the scaffolds, 105 rMSC were loaded on each scaffold for an hour and cultured in 1 ml medium. After day 5 the medium was discarded. The cells/scaffolds were washed once with 1 ml PBS. The cells were fixed in 4% paraformaldehyde (PFA) for 30 minutes at 37°C and rinsed with 1 ml distil water. The scaffolds were air dried at room temperature overnight. The cells attachment on the scaffolds were observed using field emission scanning electron microscopy (SEM).

Characterization

The morphology of the porous scaffolds was examined with a scanning electron microscope (SEM, Nova NanoSEM-450) operated at low vacuum mode at 50 Pa. Low vacuum detector was attached with its cone under pole piece. X-ray diffraction (XRD) was performed on XPERT-PRO Diffractometer, operated at 40 kV and 40 mA using Cu K_{α} radiation. The detector was scanned over a range of 2θ angles from 20° to 70° with a step size of 0.02°. FT-IR (Thermo-Nicolet 6700 P Spectrometer (USA)) was taken in the wave number range of 500 cm^{-1} to 4000 cm^{-1} in the photo-acoustic mode in the resolution of 8 cm^{-1} with 256 numbers of consecutive scans.

3. Results and discussion

SEM microstructure of fabricated scaffolds

Figs. 1-4 show the morphologies of the freeze dried composites of nCHA, $\text{Ca}_{10}(\text{PO}_4)_6\text{-(CO}_3)_y(\text{OH})_2$ with $y=0,2,4$, with various polymers such as with GE (Fig.1a,b, c), PVA (Fig. 2a,b,c), CS (Fig. 3a,b,c), and PVA-CS (Fig. 4a,b,c), respectively. In all these Figures (1-4), a, b, c, represent the micrographs for the composites made of nCHA having carbonate component $y=0, 2$, and 4, respectively. The analysis of all these twelve SEM micrographs (Figs. 1-4) clearly suggests that both the parameters, the changing concentration of carbonate (y values) and the polymers used (GE, PVA, CS, CS and PVA), impact the morphology of the pore, interconnectivity and their respective sizes. These effects are summarized in Table 1.

In the case of GE/nCHA, for $y=0$, scaffolds, as shown in Fig. 1(a), the pores are large in diameters, from 150 to 200 μm . and interconnected. Whereas for the same polymer GE but with higher value of y ($=2$), Figure 1(b), the composite structure shows less porosity and the pore size decreases significantly, varying in the range of 5-20 μm . With the same polymer, GE, but for $y=4$, the scaffolds, the pore sizes get larger, 250 to 400 μm , and they show good interconnectivity as well, Fig.1c. The shape of the pores also gets regular spherical. The SEM micrographs for PVA/nCHA with $y=0,2,4$ composites are shown in Figures 2(a), 2(b) and 2(c), respectively. By

changing the polymer from GE to PVA, a significant change in the morphology of the scaffolds is observed especially in the pore shape and sizes. The pores shape is no longer spherical. It has become elongated and the sizes vary from (5-10 μm), (5-20 μm) and (5-200 μm), for $y=0,2$, and 4 respectively. Good pore interconnectivity is also observed in these composites with PVA. In the case of CS/nCHA ($y=0, 2, 4$) composite scaffolds, the pore size of that scaffolds varies from 10-100 μm as shown in Figure 3(a), 5-20 μm in Figure 3(b) and 10-80 μm in Figure 3(c). SEM images of PVA/CS/nCHA composite scaffolds are shown in Figures 4(a), 4(b) and 4(c), with the pore size ranging from 2-8 μm , 5-20 μm and 10-100 μm respectively. In these two cases for different polymer and their combination, CS and CS-PVA, the morphologies also noticeably change for different values of $y= (0, 2, 4)$ as well as for GE and PVA.

In general, it is observed in all the samples the pore size increases when the value of “ y ” is changed from 0 to 4 (i.e. increased carbonate content in HA lattice). The SEM micrographs also show that nCHA is uniformly distributed in the polymeric matrix. All the samples show high porosity, however, for almost all the polymer used, the optimum pore size required for bone cell growth[10] is found best in the case of GE/nCHA with $y=4$.

Table 1: SEM Pore size range of freeze drying scaffolds

Composite Scaffold of nCHA with Polymer	Value of $Y \text{ Ca}_{10}(\text{PO}_4)_6 \cdot y(\text{CO}_3)(\text{OH})_2$	Pore Size Range(μm)
Gelatin	0	150-200
PVA	0	5-10
Chitosan	0	10-100
Chitosan and PVA	0	2-8
Gelatin	2	2-20
PVA	2	5-20
Chitosan	2	5-20
Chitosan and PVA	2	5-20
Gelatin	4	250-400
PVA	4	5-200
Chitosan	4	10-80
Chitosan and PVA	4	10-100

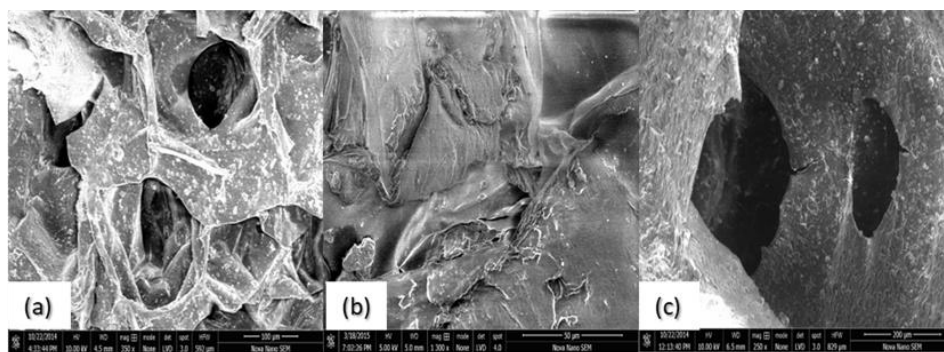


Fig. 1. Freeze dried scaffolds of Gelatin with nCHA for (a) $Y=0$ (b) $Y=2$ and (c) $Y=4$

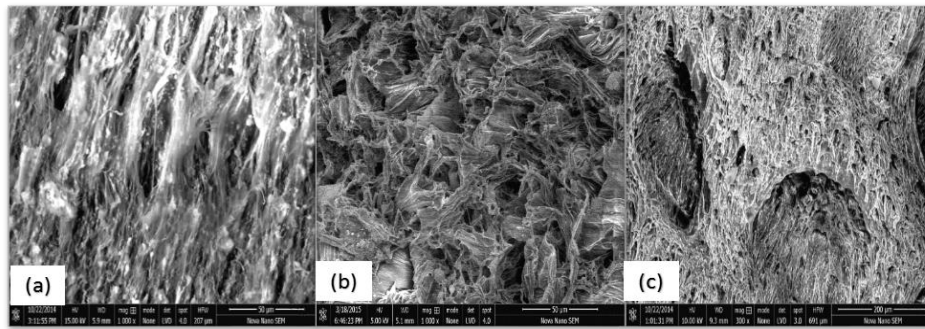


Fig. 2. Freeze dried scaffolds of PVA with nCHA for (a) $Y=0$ (b) $Y=2$ and (c) $Y=4$

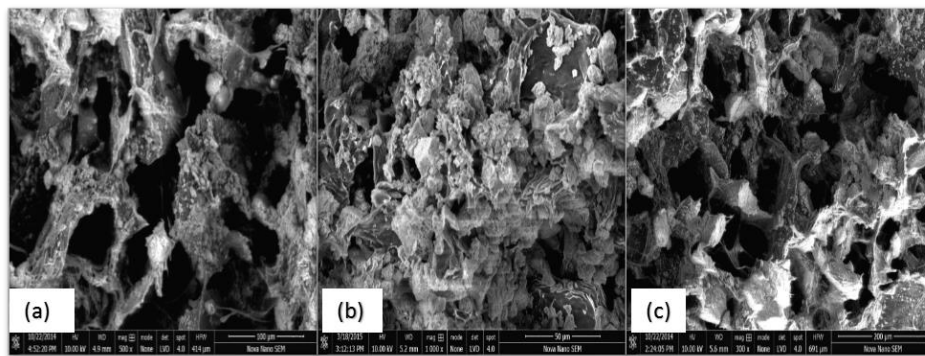


Fig. 3. Freeze dried scaffolds of Chitosan with nCHA for (a) $Y=0$ (b) $Y=2$ and (c) $Y=4$

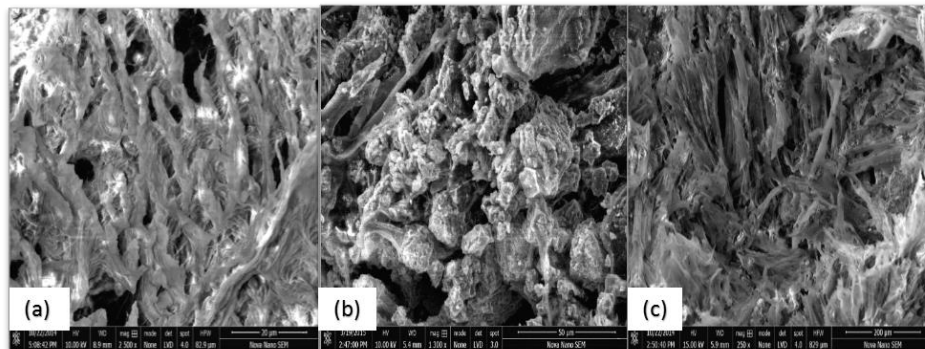


Fig. 4. Freeze dried scaffolds of Chitosan and PVA with nCHA for (a) $y=0$ (b) $y=2$ and (c) $y=4$

XRD Analysis

X-Ray diffraction data was collected for all samples in order to assess the phase purity, crystallinity, and are represented in three sets of Figures 5, 6, 7. In each set of Figs. (5, 6, 7), 'a' represent the patterns for starting nCHA with varying amount of carbonate, $y=0, 2, 4$. The patterns in Figure 5(a), 6(a) and 7(a) give a good match with the line pattern of phase-pure HA (ICDD pattern 09-0432)[24]. The XRD patterns with the addition of different polymers (GE, PVA, CS) into nCHA are shown in Figures 5, 6 and 7 (b,c,d,e), respectively. These patterns look similar and exhibit less crystallinity due to the presence of the polymer. Nevertheless, CHA does not lose crystallinity after treating with different polymers to make composite scaffolds. The main HA peak formed at about 32° (2θ) on all the polymers is seen in all the XRD patterns.

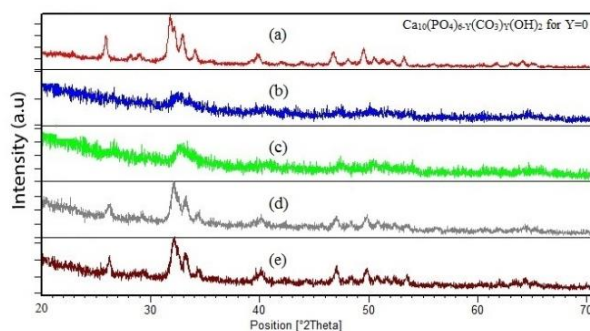


Fig. 5. XRD of a) nCHA, $Ca_{10}(PO_4)_6-y(CO_3)_y(OH)_2$ for $y=0$, Freeze dried scaffolds of nCHA $y=0$ and b) Gelatin, c) PVA, d) Chitosan, e) PVA and Chitosan

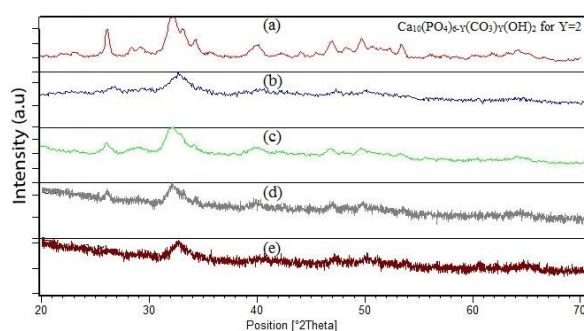


Fig. 6. XRD of a) nCHA, $Ca_{10}(PO_4)_6-y(CO_3)_y(OH)_2$ for $y=2$, Freeze dried scaffolds of nCHA with $y=2$ and b) Gelatin, c) PVA, d) Chitosan, e) PVA and Chitosan.

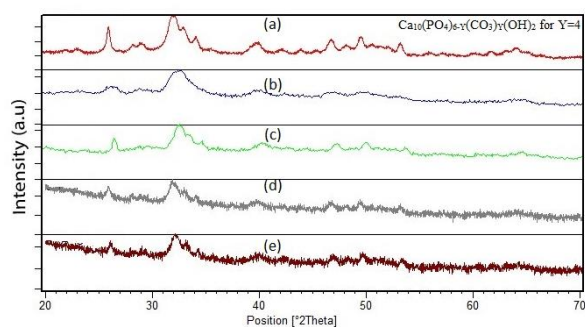


Fig. 7. XRD of a) nCHA, $Ca_{10}(PO_4)_6-y(CO_3)_y(OH)_2$ for $y=4$, Freeze dried scaffolds of nCHA with $y=4$ and b) Gelatin, c) PVA, d) Chitosan, e) PVA and Chitosan

FT- IR Analysis

FTIR analysis of prepared freeze-drying scaffolds was employed to determine the nature of the chemical bonding due to any chemical process. Figures 8, 9 and 10 represent the results of nCHA for $y=0, 2, 4$ respectively with the used polymers (GE, PVA and CS) and Table 2 gives the information of peaks as assigned to the various kinds of chemical bonds found in these spectra. Figures 8(e), 9(e), 10 (e), for the spongy samples prepared from nCHA powders with $y=0, 2,$ and $4,$ respectively, show peaks at 3569 and 622 (cm^{-1}) corresponding to stretching mode (ν_s) and liberation mode (ν_L) of hydroxyl group of HA-Lattices. The bands in the range of $1350-1525$ correspond to asymmetric stretching (ν_3) of the C–O bond in HA. The band from 1026 to 1100 cm^{-1} corresponds to asymmetric stretching modes (ν_3) of the P–O bond of phosphate and the Peak at 961 cm^{-1} corresponds to the symmetric stretching mode (ν_1) of the P–O bonds of phosphate. In

Figure 8(e), 9(e) and 10(e) the peaks at 876 cm^{-1} correspond to the bending mode (ν_2) of the O–C–O linkage of carbonate in HA.[25]

Gelatin-nCHA for $y=0, 2$ and 4 composite scaffolds as characterized by FTIR are shown in Figures 8 (a), 9(a) and 10(a), respectively. The pattern shows the mixed composition of GE and nCHA at the weight ratio of $1/1$. It was observed that amide band derived in the spectra and the peaks like $1235, 1660, 1548, 2934, 3046\text{ cm}^{-1}$ is due to Gelatin in carbonated HA lattices,[1] which are described in Table 2. The C = O stretching at $1600\text{--}1670\text{ cm}^{-1}$ for the amide I and N-H bending at $1500\text{--}1600\text{ cm}^{-1}$ for the amide II also indicate the presence of GE in scaffolds from the literature [16]. The shift of band at 1334 cm^{-1} in GE indicates the confirmation of chemical bond formation between carboxyl ion in GE and nCHA lattices phases [15, 16]. During the process of nCHA-GE composite, the Ca^{2+} ions will make a covalent bond with Ca-COO^- ions of GE molecules [26]. Furthermore, this cross-linking process indicates the strong chemical bonding between the GE and nCHA. The nCHA particles provide the binding ability and are eventually entrapped into the gelatin network.

The FTIR spectra of PVA-nCHA for $y=0, 2$ and 4 composite scaffolds are shown in Figures 8(b) and 9(b) and 10(b) respectively. The patterns show the mixed composition of PVA and nCHA at the weight ratio of $1/1$. Some characteristic peaks are the same as observed in the nCHA pattern but due to addition of PVA an extra peak was observed. The characteristic broad band in the range of 3100 to 3700 cm^{-1} is the stretching mode of OH^- ions which is due to strong hydrogen bond of intra-molecular and intermolecular type[27]. The characteristic absorption band of PVA occurs at 2926 cm^{-1} and is due to asymmetric stretching of CH_2 while the band at 2907 is due to symmetric stretching of CH_2 [28].

The FTIR spectra of Chitosan-nCHA for $y=0, 2$ and 4 composite scaffolds are shown in Figures 8(c) and 9(c) and 10(c) respectively. The patterns show that the composition is a mixture of CS and nCHA for the weight ratio of $1/1$. Due to the addition of CS, these FTIR spectra show the additional peaks for amide groups of CS, as provided in Table 2. The band observed at 1738 cm^{-1} is due to carbonyl group (C=O) of Chitosan, C–H stretching and bending observed at 1415 cm^{-1} and 1360 cm^{-1} , respectively, and the stretching mode at 1153 cm^{-1} is due to amine stretching mode (ν_s) N–H[17]. The peaks observed at 1077 cm^{-1} and 1030 cm^{-1} correspond to (C–O–C) stretching mode and the absorption bands of the amide I and amide II groups at 1650 and 1566 cm^{-1} , respectively[29].

The FTIR spectra of PVA-Chitosan-nCHA for $y=0, 2$ and 4 , composite scaffolds are shown in Figures 8(d), 9(d) and 10(d) respectively. The patterns show the mixed composition of PVA, CS and nCHA at the weight ratio of $(1:1:2)$. Due to the presence of two polymers (PVA and CS) with nCHA. These 'd' patterns appear as if they are combination of 'b', 'c', and 'e' patterns contained in Figures 8, 9 and 10 and show all the characteristic peaks appearing in their individual patterns.

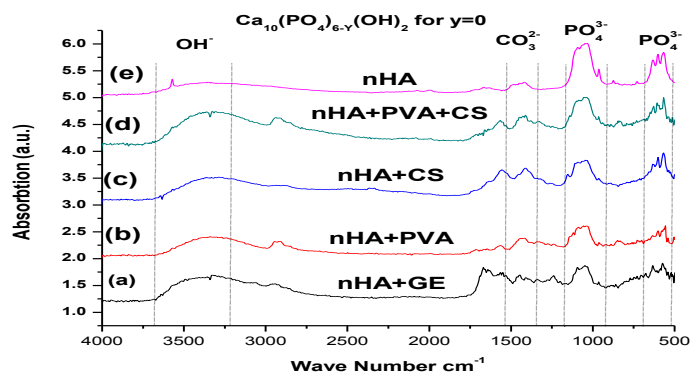


Fig. 8. FTIR spectra of freeze dried scaffolds of nCHA for $y=0$ with a) Gelatin, b) PVA, c) Chitosan, d) PVA and Chitosan and e) nCHA for $y=0$

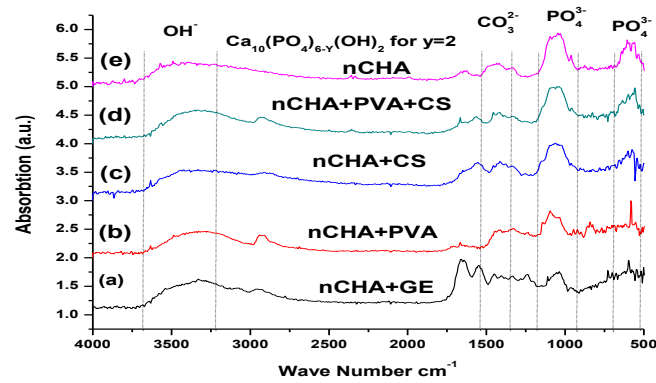


Fig. 9. FTIR spectra of freeze dried scaffolds of nCHA for $y=2$ with a) Gelatin, b) PVA, c) Chitosan, d) PVA and Chitosan and e) nCHA for $y=2$

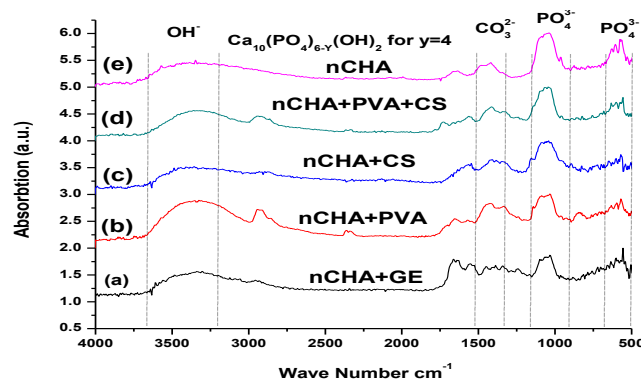


Fig. 10. FTIR spectra of freeze dried scaffolds of nCHA for $y=4$ with a) Gelatin, b) PVA, c) Chitosan, d) PVA and Chitosan and e) nCHA for $y=4$

Table 2. information of peaks appearing in FTIR spectra from Figures 8, 9 and 10

Compound	Peak list Wavenumber (cm ⁻¹)	Chemical bonding
HA	1026-1100, 561, 601, 963	Phosphate Bend (PO ₄)
HA	3569,622	Hydroxyl Group (OH)
HA	876, 1417, 1460	Carbonate bend(CO ₃)
(GE) amide III	1235	N-H bend
GE-HA	1344	Ca-COO
(GE) amide I	1600-1670	C=O stretching
GE) amide II	1550-1600	N-H bending
GE	3100-3680	O-H stretching
(GE)Amide B	2934, 3046	C-H starch
PVA	3100-3700	O-H stretching
PVA	2926,2907	stretching of CH ₂
Chitosan	1738	carbonyl group (C=O)
Chitosan	1415	C-H stretching
Chitosan	1360	C-H bending
(Chitosan) amide	1153	N-H stretching
Chitosan	1030, 1077	(C-O-C) stretching
Chitosan	1566	COO ⁻ stretching (amide II)
Chitosan	1650	Amide I

MTT Assay to demonstrate cell compatibility to scaffolds

We employed MTT assay to determine the rMSC viability after 7 days of growth with samples having different compositions and ratios (PVA+nCHA, Gel. + nCHA, CS+nCHA and CS+nCHA+PVA) and compared their viability with control cells, grown without any samples in a well (TCP), as shown in Figure 11. Our results suggest that these compositions don't show significance difference in viability of rMSC compared with control. Furthermore, our data implies that none of the composition analyzed affected the viability and proliferation capacity of the rMSC compared with control.

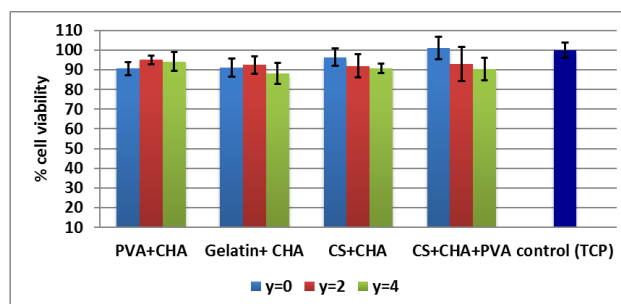


Fig. 11. %Viability of rat mesenchymal stem cells (rMSC) seeded in control in (tissue culture plate: TCP) (without sample), with poly vinyl acid + carbonated hydroxyapatite (PVA+nCHA), Gelatin + nCHA, chitosan (CS) + nCHA, CS + nCHA + PVA. All composition with tested for $Y=0,2,4$, values. The viability of the cells was determined by MTT assay after 7days of culturing. Bars represent mean cell viability normalized to control cells and error bars depict the standard deviation of three independent experiment ($n=3$)

Cell Attachment

SEM analyses were carried out to investigate the rMSC attachment on all the samples. It is observed that the cells adhere well to surface of all the samples (Figure 12). Altogether the SEM data suggest that rMSC can attach and spread on all the compositions in this study.

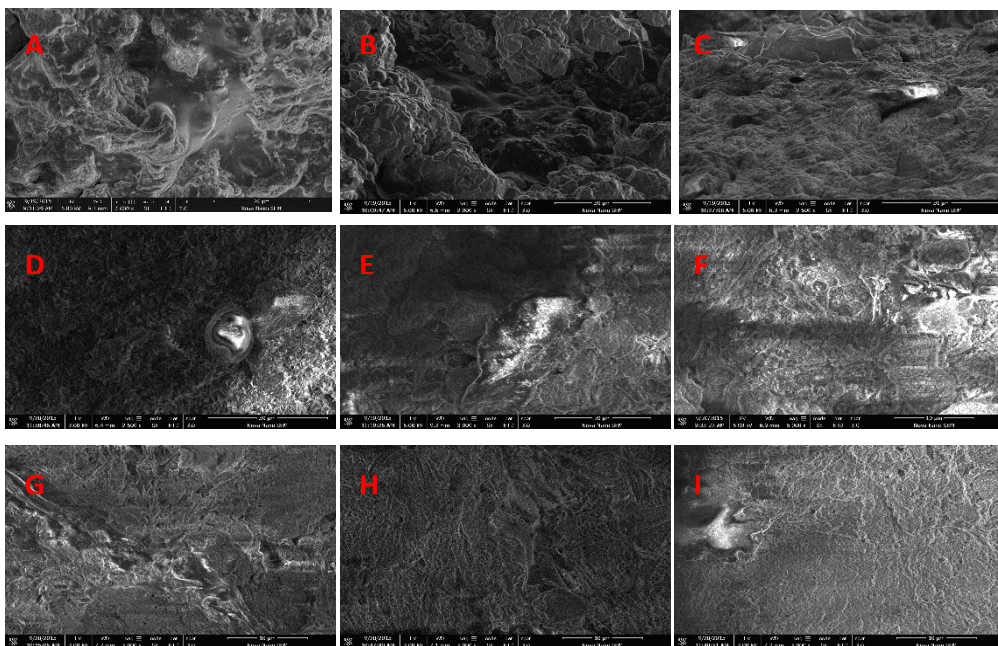


Fig. 12. SEM micrographs of rMSC attachment on PVA+nCHA ($y=0, 2, 4$) samples are shown in image A, B and C, respectively. CS+nCHA ($y=0, 2, 4$) are shown in image D, E and F respectively. CS+nCHA+PVA ($y=0, 2, 4$) are shown in image G, H and I respectively. These micrographs were taken on day 4 of culturing the cells with the scaffolds.

4. Conclusions

CHA nanoparticles $[\text{Ca}_{10}(\text{PO}_4)_6(\text{CO}_3)_y(\text{OH})_2]$ with $y=0, 2, 4$, were successfully prepared through hydrothermal method using the common precursor materials such as $[\text{Ca}(\text{NO}_3)_2 \cdot 4\text{H}_2\text{O}]$, $[(\text{NH}_2)_2\text{CO}]$ and $[(\text{NH}_4)_2\text{HPO}_4]$ with control over solution pH, temperature and Ca:P ratio. We developed nCHA/gelatin, nCHA/PVA, nCHA/CS and nCHA/PVA/CS composite scaffolds by freeze drying method to increase the bioactivity of bone material for bone tissue engineering. The morphology of the composite scaffolds shows porous structure and good interconnectivity that is suitable for bone growth and regeneration. The pore size increases with increased carbonate content in nCHA for $y=2$ and 4. Comparing the microstructure of all the freeze-dried composites prepared with different polymers, it is evident that polymer GE shows the lowest porosity, as evidence from the surface area measurements (Supplementary data) as compared with the microstructures obtained with other polymers. We have demonstrated to a certain degree control over general porosity of nCHA-polymer composite through polymer selection. The XRD and FTIR analyses confirmed the phase purity of the nano sized apatite, nCHA, used. We have shown that nCHA and polymer used present a bioactive material explorable for tissue engineering application.

Acknowledgements

We are grateful to HEC, Govt. of Pakistan, for providing funds under NRP project No. 1835 and HEC Mega PC-1 and Most P-1 of Government of Pakistan.

References

- [1] M. Azami , F. Moztaezadeh , M. Tahriri, Journal of Porous Materials **17**(3), 313 (2010)
- [2] J. Barralet , S. Best , W. Bonfield, Journal of biomedical materials research **41**(1), 79 (1998)

- [3] D.S.K. Garg, *Journal of Bone Reports and Recommendations*
- [4] A.C. Jones , C.H. Arns, D.W. Hutmacher, B.K. Milthorpe, A.P. Sheppard, M.A. Knackstedt, *Biomaterials* **30**(7), 1440 (2009)
- [5] D.W. Hutmacher, *Biomaterials* **21**(24), 2529 (2000)
- [6] S. Haque , I. Rehman , J.A. Darr, *Langmuir* **23**(12), 6671 (2007)
- [7] I. Manjubala , S. Scheler , J. BöSSERT , K.D. Jandt, *Acta Biomaterialia* **2**(1), 75 (2006)
- [8] A.S. Clasen , I. Ruyter, *Advances in Dental Research* **11**(4), 523 (1997)
- [9] W. Suchanek , M. Yoshimura, *Journal of Materials Research* **13**(01), 94 (1998)
- [10] M.C. Chang , C.-C. Ko , W.H. Douglas, *Biomaterials* **24**(17), 2853 (2003)
- [11] L. Kong , Y. Gao , W. Cao , Y. Gong , N. Zhao , X. Zhang, *Journal of Biomedical Materials Research Part A* **75**(2), 275 (2005)
- [12] P.X. Ma , R. Zhang, G. Xiao, R. Franceschi, *Journal of biomedical materials research* **54**(2), 284 (2001)
- [13] S.C. Rizzi , D. Heath , A. Coombes , N. Bock , M. Textor , S. Downes, *Journal of biomedical materials research* **55**(4), 475 (2001)
- [14] H.R. Lin , Y.J. Yeh, *Journal of Biomedical Materials Research Part B: Applied Biomaterials* **71**(1), 52 (2004)
- [15] M.C. Chang , T. Ikoma , M. Kikuchi , J. Tanaka, *Journal of Materials Science Letters* **20**(13), 1199 (2001)
- [16] M.C. Chang , J. Tanaka, *Biomaterials* **23**(24), 4811 (2002)
- [17] J. Venkatesan , Z.-J. Qian , B. Ryu , N.A. Kumar , S.-K. Kim, *Carbohydrate Polymers* **83**(2), 569 (2011)
- [18] S. Liao, W. Wang, M. Uo, S. Ohkawa, T. Akasaka, K. Tamura, F. Cui, F. Watari, *Biomaterials* **26**(36), 7564 (2005)
- [19] L. Kong , Y. Gao , G. Lu , Y. Gong , N. Zhao , X. Zhang, *European Polymer Journal* **42**(12), 3171 (2006)
- [20] D. Zhang, J. Duan, D. Wang, S. Ge, *Journal of Bionic Engineering* **7**(3), 235 (2010)
- [21] L. Ciocca, I. Lesci, O. Mezzini, A. Parrilli, S. Ragazzini, R. Rinnovati, N. Romagnoli, N. Roveri , R. Scotti, *Journal of Biomedical Materials Research Part B: Applied Biomaterials*, (2015)
- [22] S. A. Siddiqi, F. Manzoor, A. Jamal, M. Tariq, R. Ahmad, M. Kamran, A. Chaudhry, I. Rehman, *RSC Advances* **6**(39), 32897 (2016).
- [23] X. Li , Y. Zhang, G. Qi, *Cytotechnology* **65**(3), 323 (2013)
- [24] M. Wei , J. Evans, T. Bostrom, L. Grøndahl, *Journal of materials science: materials in medicine* **14**(4), 311 (2003)
- [25] A.A. Chaudhry , J.C. Knowles , I. Rehman , J.A. Darr, *Journal of Biomaterials Applications* **28**(3), 448 (2013)
- [26] M.K. Narbat , F. Orang , M.S. Hashtjin , A. Goudarzi, *Iranian Biomedical Journal* **10**(4), 215 (2006)
- [27] V. C. Costa , H. S. Costa , W. L. Vasconcelos, M. D. M. Pereira, R.L. Oréfice, H.S. Mansur, *Materials Research* **10**(1), 21 (2007)
- [28] L. Nie , D. Chen , J. Suo , P. Zou , S. Feng , Q. Yang , S. Yang , S. Ye, *Colloids and Surfaces B: Biointerfaces* **100**, 169 (2012)
- [29] J.M. Oliveira , M.T. Rodrigues , S.S. Silva , P.B. Malafaya , M.E. Gomes , C.A. Viegas , I. R. Dias , J. T. Azevedo , J. F. Mano , R.L. Reis, *Biomaterials* **27**(36), 6123 (2006).